UNIVERSITY OF CALIFORNIA, IRVINE

Demystifying the Choroid Plexus

THESIS

submitted in partial satisfaction of the requirements
for the degree of

MASTER OF SCIENCE

in Biomedical Engineering

by

Esmeralda Romero Lorenzo

Thesis Committee:
Professor Edwin Monuki, Chair
Professor Michelle Digman
Professor Wendy Liu

2020

TABLE OF CONTENTS

LIST OF FIGURES

LIST OF TABLES

ACKNOWLEDGMENTS

I would like to dedicate this work to everyone who has made it possible. I would like to begin by thanking the members of the Monuki Lab. Dr. Monuki thank you for believing in me and taking me on as a student. You were not just a PI, but a mentor and a role model. You make those around you better. With your support, I have grown as a scientist and a human. Working for you was a privilege. Brett Johnson, PhD thank you for being a beacon of light and always encouraging me to press forward and pursue science, even when the results were not favorable. I will never forget how you always managed, motivated, and inspired your army of undergraduates. I hope one day I can lead like you. Michael Neel, I would like to thank you for being a wonderful colleague and friend. Thank you for always finding the best antibodies.

Second, I would like to thank Professor Digman, Professor Liu and Professor Lopour. Without your support I would not be writing this manuscript. Thank you for allowing me to pursue higher education and thank you for expanding my knowledge of bioengineering. I thoroughly enjoyed learning from your lectures and seminars, and am extremely grateful for you feedback during my graduate studies.

Lastly, I would like to thank my family and friends. Mom and Dad, thank you for your love and unconditional support. Marco, thank you for being the best friend and brother that I could have asked for. David, thank you for always being present and helping me achieve my dreams, and thank you to all of my friends who directly and indirectly rooted for me along the way.

ABSTRACT

Demystifying the Choroid Plexus

By

Esmeralda Romero Lorenzo

Master of Science in Biomedical Engineering

University of California, Irvine, 2020

Professor Edwin Monuki, Chair

As biomedical technology advances and studies uncover new forms of elucidating the underlying mechanisms of our brain, we can begin to study the brain's components, development, function, and health. This thesis will focus on the choroid plexus (CP), a tissue essential for the development and maintenance of the brain. The choroid plexus is composed of cuboidal epithelial cells known was choroid plexus epithelial cells (CPEC). CPEC are responsible for cerebrospinal fluid (CSF) secretion and form the blood cerebrospinal fluid barrier. Over and under production of CSF production have been linked to various mental disorders. Furthermore, it has been speculated that accelerated CPEC atrophy leads to a reduction in CSF and protein secretion, a phenomenon described in Alzheimer's Disease (AD). Despite CPEC's critical role, very little has been done to study the normal CPEC function. In this thesis, CPEC morphology, protein expression, and barrier properties will be explored. This body of work aims to demystify normal CPEC function in hopes that it will serve as foundation for future pathological studies.

CHAPTER 1: Introduction

1.1 The Choroid Plexus and Its functional Role in the Brain

The last century has revolutionized how we view and study the world around us. Due to vast technological leaps, we are now equipped to study even the most complex enigmas of our world, including the very one that is most dear to us human, our brain. As biomedical technology advances and studies uncover new forms of elucidating the underlying mechanisms of our brain, we can begin to study the brain's components, development, function, and health. This thesis will focus on the choroid plexus (CP) which is essential for the development and maintenance of the brain.

The choroid plexus, a secretory tissue found in the ventricles of the brain, is responsible for the production of cerebral spinal fluid (CSF). In normal adults, the total CSF is estimated to be 100-150ml. It is replaced three to four times a day, suggesting that the choroid plexus produces approximately 500ml of CSF a day(Barkho & Monuki, 2015). The CSF is a major source of entry for substances like calcium and hormones, such as insulin-like growth factor-II and transthyretin(Vieira et al., 2015). It also functions as a filtering system. Thus, the CSF keeps the brain nourished by circulating nutrients and waste-free by removing metabolic wastes. Given the CSF's vital function, it is imperative that the choroid plexus produces the appropriate amount of CSF. It has been speculated that accelerated CP atrophy leads to a reduction in CSF and protein secretion, a phenomenon observed in patients with Alzheimer's Disease (Suzuki et al., 2015). The overproduction of CSF has also been linked to detrimental effects, such as hydrocephalus which applies pressure to the brain and can cause brain damage(Javed & Lui, 2019).

The choroid plexus also plays another vital role in the brain. The choroid plexus epithelium separates blood vessels from the CSF and the brain. This interphase between the central nervous

system and circulatory system is known as the blood cerebrospinal fluid barrier (BCSFB). The BCSFB regulates pathogen access to the brain.

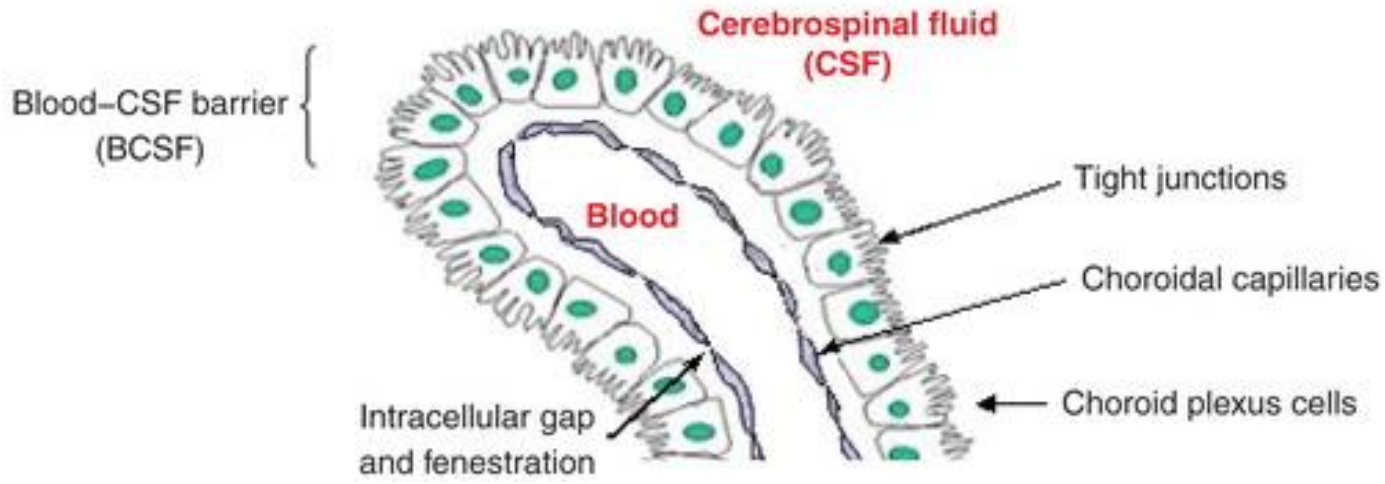

Figure 1.1 Overview of the blood cerebrospinal fluid barrier (BCSFB).(Zhao et al., 2013)

In order for viruses, bacteria, fungi, and other parasites to gain passage to the central nervous system, they can cross the blood cerebrospinal fluid barrier(Mastorakos & McGavern, 2019). Concurrently, the BCSFB grants access to leukocytes that counteract the foreign substances and diseases(Johanson & Johanson, 2018). Despite the BCSFB's reactive and proactive role in regulating the brain health and maintaining homeostasis, the mechanisms by which this regulation occurs remains a mystery.

To shed light on these mysterious mechanisms, this thesis will study the cellular morphology of the choroid plexus in a CPEC reporter mouse model. To begin, this work will provide background on the first studies of the choroid plexus. It will touch on the location, structure, and the key cell type of the choroid plexus - choroid plexus epithelial cells (CPEC). During this study, it was revealed that CPEC are highly heterogeneous. Thus, this work will focus on the CPEC's heterogeneity and delve into methods of studying cell heterogeneity in mice.

Lastly, it will explore the findings of this study and the highlight potential future works, which can help further demystify the choroid plexus.

1.2 Clinical Significance

The choroid plexus is crucial to the brain's well-being. This section will focus on the clinical significance of this tissue and the multiple neurological disorders that it is involved in. As previously mentioned, choroid plexus atrophy has been seen in Alzheimer's disease. It has been observed that Aβ and Biondi ring tangles accumulate in the Alzheimer's disease choroid plexus.

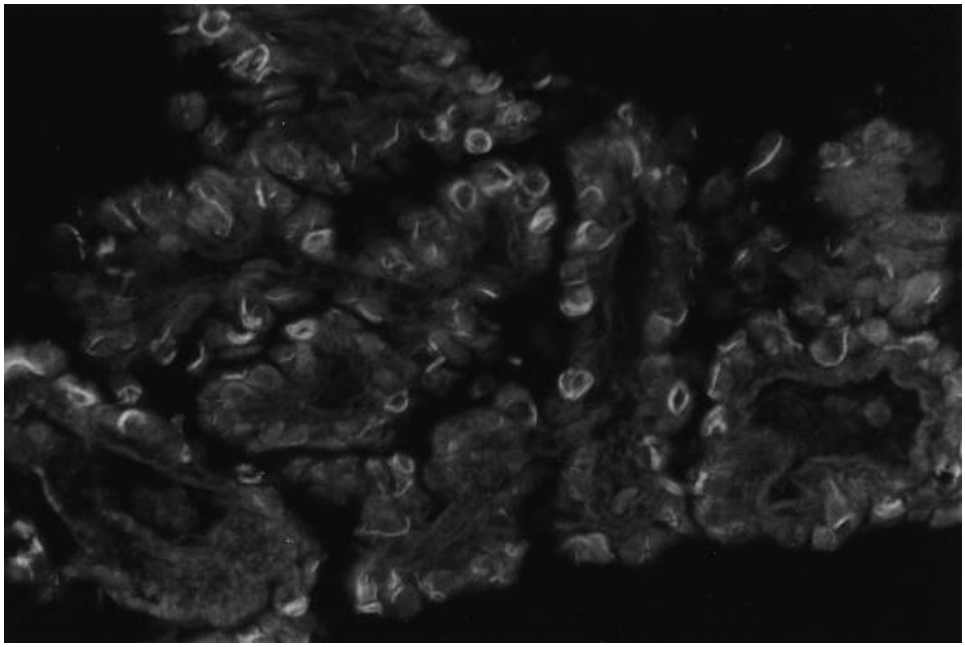

Figure 1.2 Fluorescent light micrograph Bondi Ring Tangles in the CP of the brain of a 78-year-old human female with Alzheimer's Disease (Magnification: 530×).(Wen et al., 1999)

multiple sclerosis, the choroid plexus is believed to be the entry site for lymphocytes in the CSF and brain, and for presentation of antigens. Choroid plexus papilloma and carcinoma represent the brain tumors that can occur as early as the first year of life.

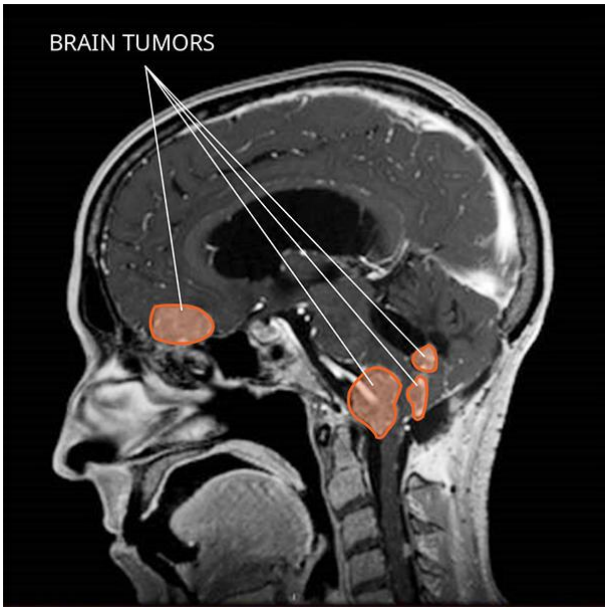

Figure 1.3 MRI of Choroid Plexus tumors in the brain. (Choroid Plexus Tumors - National Cancer Institute)

Furthermore, the choroid plexus has been linked Amyotrophic Lateral Sclerosis, Huntington disease, Schizophrenia and Parkinson disease.

CHAPTER 2: Choroid Plexus Overview

2.1 Anatomy of the Choroid Plexus

The choroid plexus can be found in the lining of each of the brain ventricles. The structure of the choroid plexus is similar across the third, fourth, and lateral ventricles. Upon initial analysis, the choroid plexus structure exposes it secretory role. On the apical side of the choroid plexus, cuboidal epithelial choroid plexus cells are localized. The CPEC has numerous microvilli and cilia that allow the choroid plexus to produce CSF. To maintain the blood cerebrospinal fluid barrier, the CPEC are linked together by tight junctions.

The CPEC surrounds the choroid plexus stroma. The choroid plexus stroma has unique properties. The stroma is comprised of large capillaries, which are composed of endothelial cells that are highly permeable due to diaphragmed fenestrations. These fenestrations allow for free exchange of fluids and molecules. These fenestrated capillaries are uncommon in the body, with two other regions of the body that exhibit similar structures being the kidney and liver.

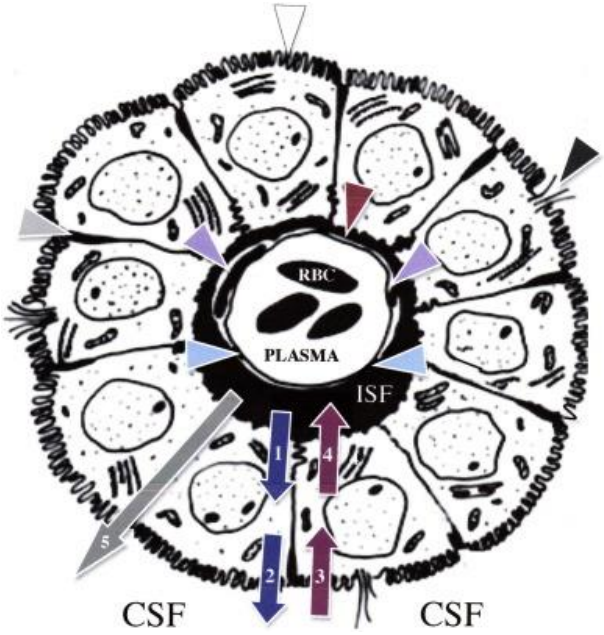

Figure 2.1 Schema of Choroid Plexus Cross Section (Spector et al., 2015)

2.2 Choroid Plexus Epithelial Cells

As previously mentioned, the choroid plexus plays a vital role in producing CSF and comprising the blood cerebrospinal fluid-brain barrier. However, not all cells and components of the choroid plexus drive these functions. The choroid plexus epithelial cells with their tight junctions and microvilli are solely responsible for the barrier properties and secretory nature of this tissue.

Furthermore, it is believed that the choroid plexus epithelial cells may function as a major entry way for immune cells into the central nervous system and could act as a potential route for drug delivery. Despite these findings, very few studies have focused on the nature of these cells. In 2019, only 27 papers referencing the CPEC as a title word were found in PubMed. Therefore, this section will focus on the main proteins found in the choroid plexus and their functions. Throughout this thesis, these proteins will be referenced and analyzed to reveal the nature of these cells.

2.3 Choroid Plexus Epithelial Cell Proteins

2.3.1 Transthyretin

Thyroid hormones (TH) are critical to brain development and must be transported to the brain during specific stages of development. During prenatal stages of life, insufficient amount of TH can lead to mental retardation. In adults, insufficient levels can lead to weight gain, fatigue, and mental disorders (Richardson et al., 2015). Thus, it is critical that TH access to the brain is regulated. The key regulator is Transthyretin (TTR). TTR is the protein responsible for transporting thyroid hormones from the blood into the CSF. In 1986, Stauder et al. discovered that TTR mRNA was synthesized in the choroid plexus, specifically in the choroid plexus epithelial cells (Stauder et al., 1986). In 1990, the Schreiber group determined that the choroid plexus was the tissue with the highest concentration of TTR per gram. Given the abundance of TTR and

specific localization of TTR in the CPEC, TTR will be the key protein used to analyze CPEC cultures in this study.

2.3.2 Aquaporin 1

In the clinical significance portion of this thesis, the dangers of over and under production of CSF were stressed. CPEC proteins are vital for maintaining CSF equilibrium. CSF is 99% water and produced in a two-step process. The first is a filtration step. Plasma must be filtered as it moves from fenestrated capillaries to the interstitial space. The fluid then needs to pass through the CPEC barrier to enter the ventricles. Current models suggest that water transport is a result of an active processes that secretes sodium, potassium, chloride, and bicarbonate ions into the ventricle lumen (Boassa & Yool, 2005). Secretion of these ions creates an osmotic pressure, and Aquaporin 1, a water channel localized in the apical side of CPEC, facilities water transport to the CSF along this osmotic gradient.

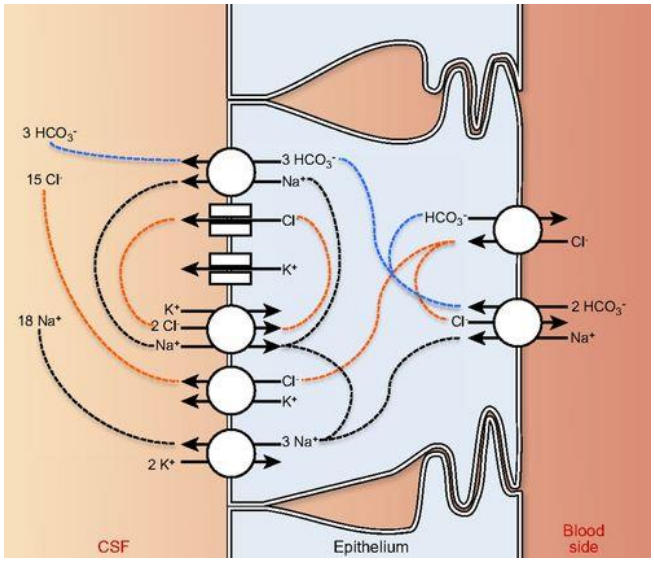

Figure 2.2 Schematic describing one of the most simplistic models of secretion. *The transcellular movement of ions is powered by the Na+-K+-ATPase, which also directly pumps solute to the cerebrospinal fluid (CSF). Net ion flux from blood side to the CSF side creates a difference in osmolarity, which drags water molecules across the epithelium, most likely mainly through aquaporin-1 in both the luminal and basolateral membranes.*

Previous Aquaporin 1 studies suggest that it functions as a gated ion channel. It is believed that ionic conductance can significantly regulate CSF secretion. Given its role in water regulation, Aquaporin 1 was incorporated in this study in hopes that Aquaporin1 expression in our new reporter primary culture will provide more information on CSF production.

2.3.3 ZO-1

One commonality between the blood-brain barrier and the blood cerebrospinal fluid barrier is the existence of tight junctions. CPEC are tightly linked through numerous tight junctions. One of the peripheral membrane proteins that is critical to tight junction regulation is ZO-1. In previous studies, ZO-1 knockdown resulted in increased leak or pathway flux (Van Itallie et al., 2009). ZO-1 also appears to have the opposite effect when it interacts with claudin-2, with a reduction in paracellular Na+ permeability being observed. Though these effects have not been observed in the choroid plexus, it is plausible that ZO-1 could regulate CPEC tight junctions, and as a byproduct, affect CSF production. Human-derived choroid plexus cells exhibited prominent TTR and ZO-1 co-expression (Watanabe et al., 2012). In this study, it is hypothesized that a similar result will be observed in the CPEC reporter mouse line.

CHAPTER 3: TTR:tdTomato CPEC Reporter Mouse Culture

3.1 TTR:tdTomato Reporter Mouse Characteristics

In order to study the CPEC characteristics, a CPEC reporter mouse model was developed in our lab. A reporter mouse is a mouse whose genome has been altered to monitor a target gene's promoter activity. Often, the coding sequence of the gene is replaced with the coding sequence of a fluorescent marker, allowing one to visualize a protein of interest. One of the most common fluorescent markers is tdTomato, which as the name suggests, fluoresces bright red. Our lab developed and characterized a TTR:tdTomato reporter mouse line to visualize and purify CPECs. This was be done by inserting a tdTomato coding sequence into a bacterial artificial chromosome (BAC) containing the human *Transthyretin* gene. Transthyretin (TTR), as previously mentioned, is the most abundant CPEC transcript and secreted protein in the CSF. It is also selectively expressed in the CPEC, thus allowing us to monitor TTR expression and visualize the CPEC.

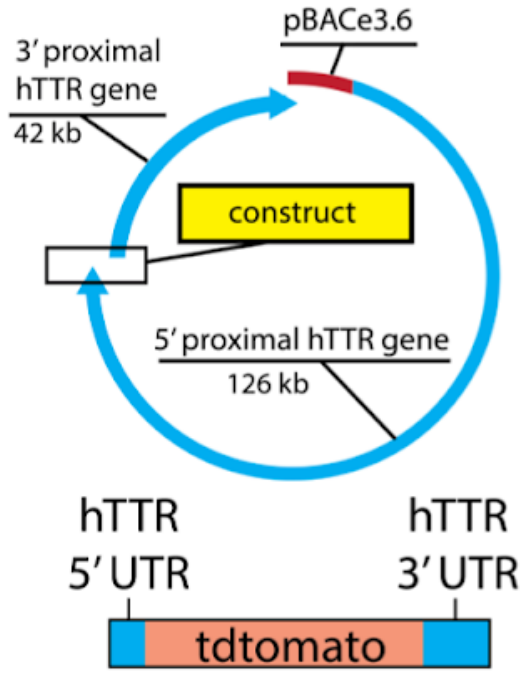

Figure 3.1 Schematic of TTR:tdTomato structure with entire sequence of human TTR gene.

3.2 Methods to Evaluate TTR:tdTomato CPEC Reporter Mouse Line

All experiments were carried out in accordance with the Institutional Animal Care and Use Committee at the University of California, Irvine. University policy and have already been reviewed and approved by the Institutional Animal Care and Use Committee (IACUC 2001-2304, AUP 16-21).

Once the tdTomato transgene was inserted into the BAC, RP11-571I2, we identified one founder line, 3154, which displayed strong fluorescence within the choroid plexus and could breed viable offspring with the same phenotypically positive characteristics. Only homozygous offspring from the 3154 line were selected and used for the present study.

3.2.1. Determining Homozygosity

The traditional PCR reaction was used to amplify the TTR:tdTomato BAC and control regions of mouse DNA. All reactions were carried out using a protocol to maximize sensitivity and specificity (Johnson et al., 2018). Finally, PCR products were separated in a 1% agarose gel and visualized under UV-light. All primers used are listed in Table 3.1.

Table 3.1 Primer Pairs to Determine CPEC Reporter line homozygosity

Primer pair	**Direction**	**Sequence (5′ to 3′)**
tdTom internal	Forward	CACCATCGTGGAACAGTACG
	Reverse	GCGCATGAACTCTTTGATGA
BAC 100 kb 5′ #1	Forward	TTAGGATTCAGGTGGCCTTG
	Reverse	TGCACATCCTTGGCAATAAA
BAC 100 kb 5′ #2	Forward	AATGAAGAGGCTGCCAAAGA
	Reverse	AGTGGATCCCACGACAGTTC
BAC 60 kb 5′	Forward	AAGCCCAAGATCAAAGCAGA
	Reverse	CTCACGTGCTGAAATCCTGA
BAC 40 kb 3′	Forward	TCAGCAGCTTCCTGCTACAC
	Reverse	GCTAGACAGGTACCCAGGGA

3.2.2 Dissection and Imaging

P21 mice were sacrificed using carbon dioxide asphyxiation followed by decapitation in accordance with IACUC guidelines. The brains were then exposed and choroid plexus from all ventricles was dissected using a stereomicroscope. The choroid plexi were submerged in phosphate-buffered saline. The unmounted, unstained choroid plexi were imaged using Nikon dissecting microscope.

3.3 TTR:tdTomato Reporter Mouse Results

At three weeks post-natal, the reporter mice expressed tdTomato and transthyretin robustly across the choroid plexus. When compared, the negative and positive littermates both appeared to be healthy and of similar size. Given that the transgenic mice were healthy, faithfully express transthyretin, and fluoresced vibrantly, these mice were used to conduct cellular studies of the choroid plexus epithelial cells. Their fluorescent nature was especially useful to purify the cells and distinguish CPEC from endothelial and other cells in culture.

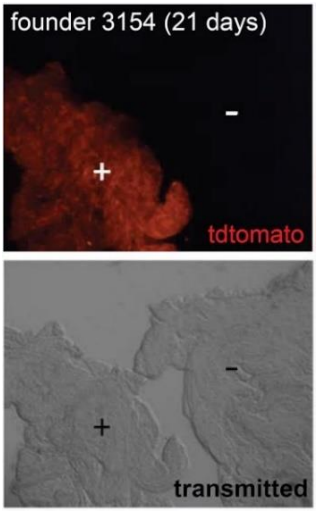

Figure 3.2 A comparison of TTR:tdTomato mouse choroid plexus with its TTR:tdTomato negative littermate. *Wet mounts of unfixed choroid plexus were imaged with a Nikon dissecting scope. The top image was taken with an RFP filter and bottom image was taken with transmitted light. From the image, it is apparent that the homozygous TTR:tdTomato positive mice fluoresces bright red and its counterpart cannot be seen.*

CHAPTER 4: Choroid Plexus Epithelial Cell Heterogeneity in vitro

4.1 Cell Morphology Heterogeneity in vitro

Heterogeneity can be found in genetically identical cells which can impact their phenotypic expressions (Altschuler & Wu, 2010). Heterogeneity in the expression of signaling molecules by the choroid plexus from different ventricles has been observed (Lun et al., 2015). This heterogeneity can be traced down to the cellular level, where differences between choroid plexus epithelial cells have been observed (Lobas et al., 2012). Understanding the various sources and types of heterogeneity in choroid plexus epithelial cells can help elucidate some of the functions of this relatively unknown tissue.

The nucleus of cells is one of the organelles whose variation could lead to cell heterogeneity. The size of the nucleus can affect cell function (Jevtić et al., 2014). It has been shown that the size of nuclei can impact chromatin condensation and ultimately gene expression (Vuković et al., 2016). In many cases the ratio of the nucleus size to cell size, or nuclear-cytoplasmic ratio, has been an important factor for determining normal cell function (Good, 2015). As such many cells have mechanisms by which the ratio remains constant even when the cells grow or shrink (Webster et al., 2009). Accurately measuring this ratio for cells in cultures therefore becomes an important factor when studying the function of these cells (Wright et al., 2008). Having viable cultures for choroid plexus epithelial cells which can allow for the measurement of this ratio is important due to the difficulty of in vivo experimentation (Gabrion et al., 1998).

With the new transgenic mouse line, CPEC cellular studies could be conducted with ease. Purifying CPEC and assessing their survival in culture became feasible. CPEC cultures were grown and nuclear and morphological studies were performed. It was revealed early on that the

CPEC in culture were highly heterogeneous and quantitative measurements were taken to support the observed characteristics.

4.2 Methods to Study Heterogeneity in vitro

4.2.1 Dissection and Cell Culture

Primary cultures of epithelial cells from mouse CPECs were prepared using the following method. 10 three-week old mice were sacrificed using carbon dioxide asphyxiation followed by decapitation per IACUC guidelines. The brains were then exposed and choroid plexus from all ventricles was dissected using a stereomicroscope. The tissue was then collected and submerged into 500 ul of PBS on ice, until the last choroid plexus was obtained. Once pooled, 500ul of collagenase II with 3mM were added to dissociate the tissue. The PBS/Collagenase II+Ca2 mixture was then put an incubator at 37C for 45 minutes. To ensure dissociation was adequate, the CPEC was mechanically dissociated by tapping the eppendorf tube every 5 minutes. The mixture was then centrifuged (3000 rpm for 3 minutes). Following centrifugation step, the pellet of cells was washed with CPEC media and resuspended. CPEC media is composed of DMEM supplemented with 10% FBS, 100 units penicillin per mL, 100 pg streptomycin per mL, and 20 µl cytosine arabinoside. Cells were maintained at 37°C, 5% CO_2 on Poly-L-lysine and laminin coated culture wells, and the medium was changed every 72 hours.

4.2.2 Immunohistochemistry

For immunocytochemical examination of ZO1 and TTR expression, CPEC cultures were washed with PBS and fixed in 4% paraformaldehyde (PFA) (30 minutes) followed by three washes with PBS. The wells were rinsed with 0.05% Triton X-100 and blocked with 1% bovine serum albumin (BSA) in PBS (45 minutes) prior to incubation with a 1:500 dilution of the primary antibody. Following incubation with the primary antibody for 60 minutes at 37°C, the cultures

were incubated in the dark with a fluorescence labeled goat anti-rabbit IgG antibody for 45 minutes at 37°C. Finally, the cells were washed in PBS solution and mounted for microscopic visualization.

4.3 Results

4.3.1 Nucleus Size in vitro

The average data across 634 nuclei in vitro taken from 40X images of P21 CPEC monolayer is shown below (Figure 4.1).

A) Average Data of 634 Nuclei

Avg. Area (Sq. Microns)	Avg. Perimeter (Microns)	Avg. Eccentricity
49.2292	25.2896	0.5685

B) 40X images of P21 CPEC monolayer to

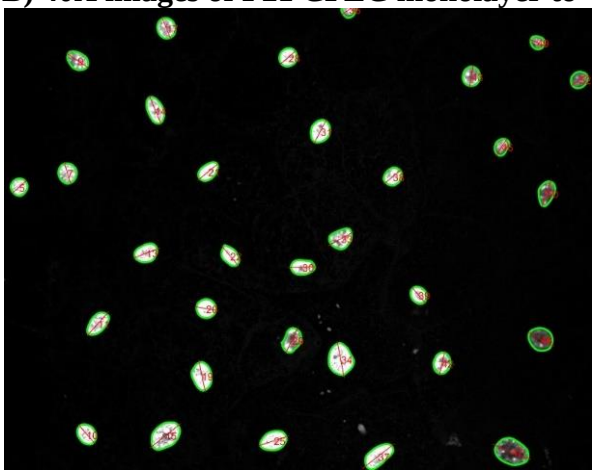

Figure 4.1 A) The table shows the average for the 634 nuclei found in the 10 images. B) One of the 10 confocal images that were used to perform nuclear analysis.

The nuclei do not appear to point in any specific direction or display widely varying eccentricities. It was also evident that the nuclei did not vary greatly in size between the cells. However, these images do not display the heterogeneity in morphology and nuclear-cytoplasmic ratio found in these cells. For that, epifluorescent imaging is needed to highlight these heterogeneities.

4.3.2 Cell Morphology

An epifluorescent image from the microscope is shown below (Figure 4.2). The Zo-1 barriers and nuclei are visible in these CPECs. There is clear heterogeneity in cell size and shape for these CPECs. The shapes and sizes include medium sized cuboidal CPECs, large irregularly CPECs, elongated CPECs, and small circular CPECs.

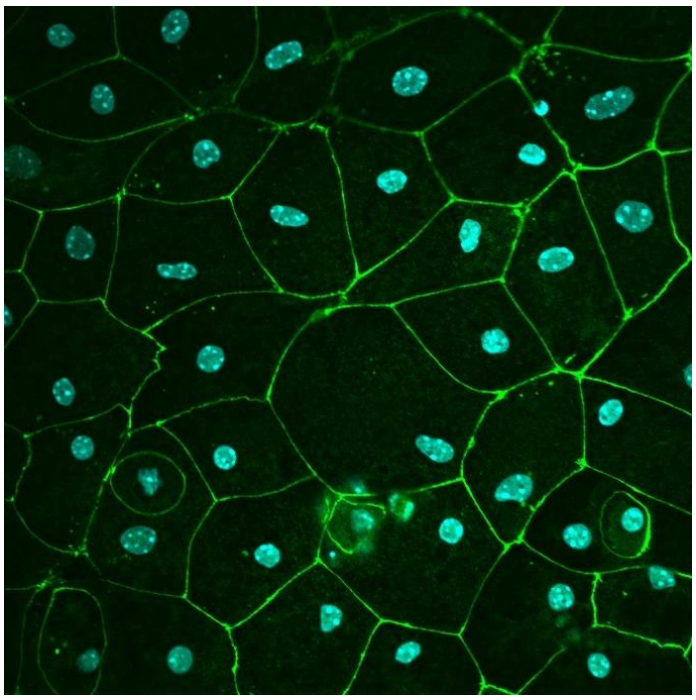

Figure 4.2 This epifluorescent image from the microscope shows the heterogeneity of the cells and distinguishes the nucleus from the cytoplasm. The cells in this image were quantitatively analyzed to determine the nuclear-cytoplasmic ratio

4.3.3 Cell Nuclear-Cytoplasmic Ratio

It appears that while the cell sizes vary greatly, nuclear sizes did not, which would indicate heterogeneity in nuclear-cytoplasmic ratios. To determine the ratio, images were processed using ImageJ. First the image was put through color thresholding to further contrast the nucleus from the cytoplasm and allow for accurate size analysis. Particle analysis was then done on all the nuclei to

determine their size. The image below shows the thresholding and particle analysis done on the image to determine relative nuclei size in pixels (Figure 4.3).

s

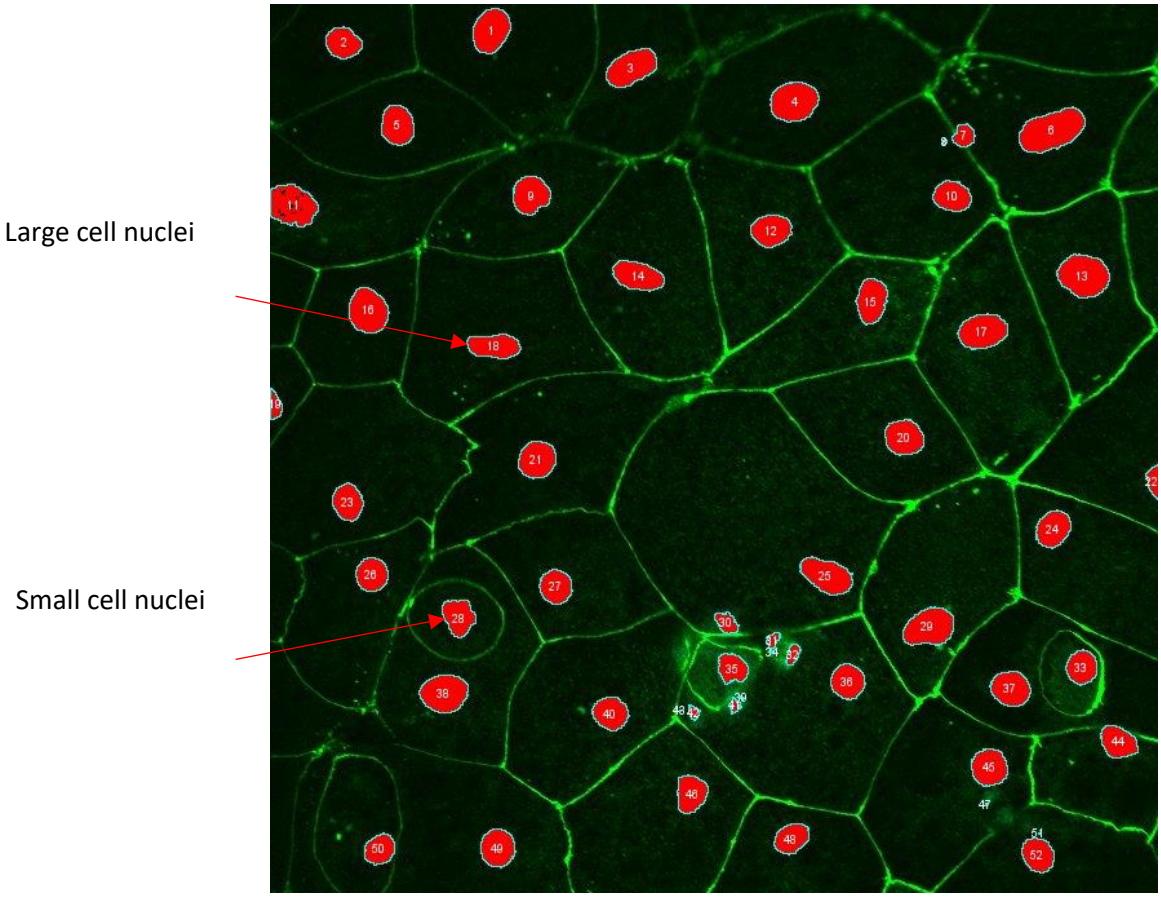

Figure 4.3 This image shows the nuclei being separated from the cytoplasm through thresholding shown in red. The areas of the red nuclei were then determine using particle analysis algorithms.

The nuclei were separated into two categories based on their morphology. The first category are small circular cells enveloped within other cells to be referred to as small cells. The second category includes the larger, mostly cuboidal cells not enveloped in other cells to be referred to as large cells. The nuclei sizes of the two categories with standard deviations are shown below (Figure 4.4)

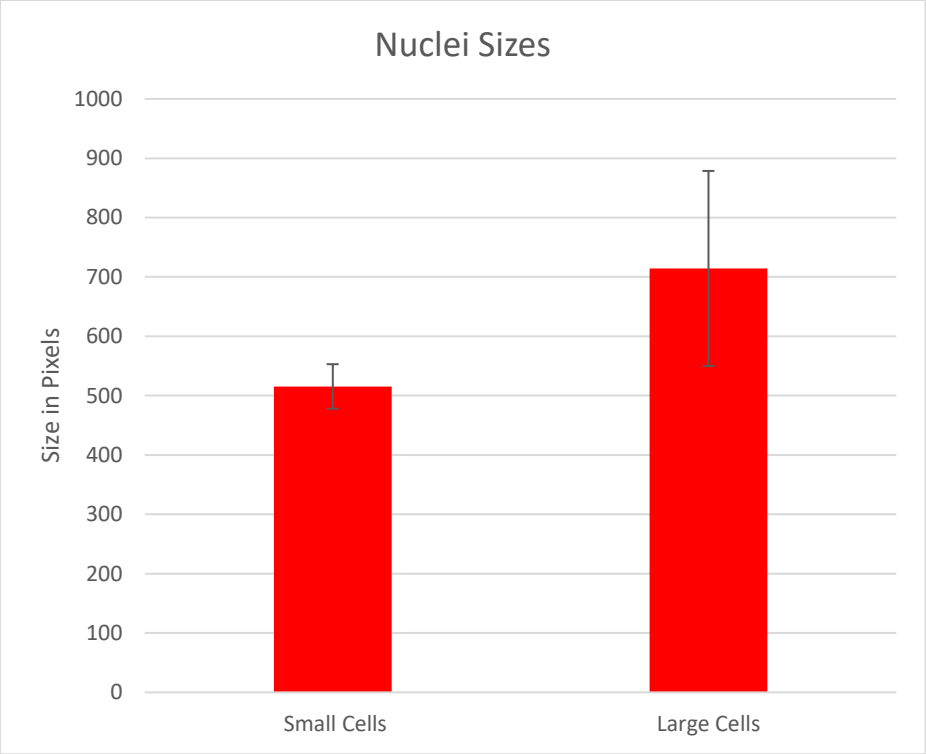

Figure 4.4 Average nuclei sizes of the two categories of cells from the image analysis

The small cell nuclei appear to be smaller than the large cells. However, when performing a paired t-test, the results were shown to not be statistically significantly ($p = 0.173$). This indicates that the nuclear sizes did not obviously differ despite the heterogeneity in morphology. The same image processing for the nuclei was then done to the cytoplasm area of the cells. However due to the cells not being fully able to be processed using the built-in algorithms, some of the cells had to be filled in manually. To ensure consistency between the manual and automatically filled in cells, cells that were automatically filled were also manually filled. When this was done there was no significant difference between the manual images and the automatically filled images. Particle analysis was then performed on the image. The image below shows the thresholding and particle analysis done on the cells (Figure 4.5).

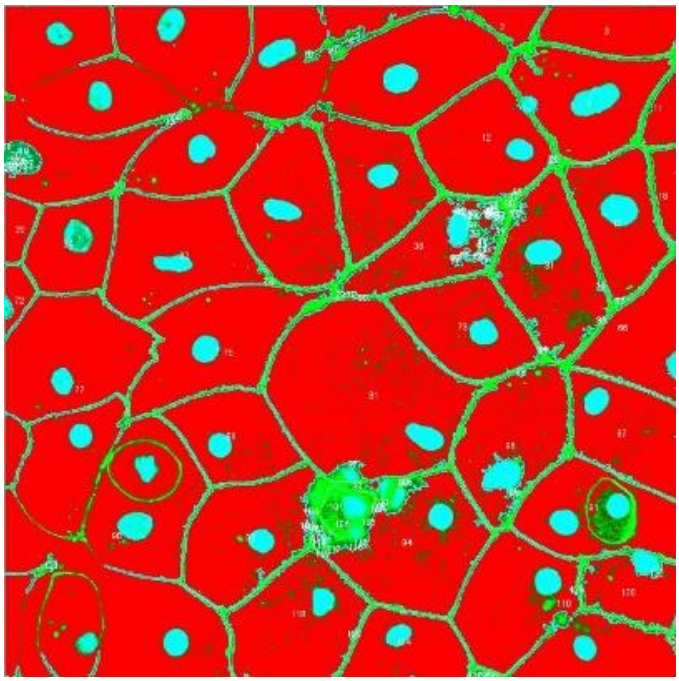

Figure 4.5 This image shows the cytoplasm being separated from the nuclei and ZO-1 barrier through thresholding shown in red. The areas of the red cells were then determine using particle analysis algorithms.

The results of the size analysis are shown in the graph below (Figure 4.6).

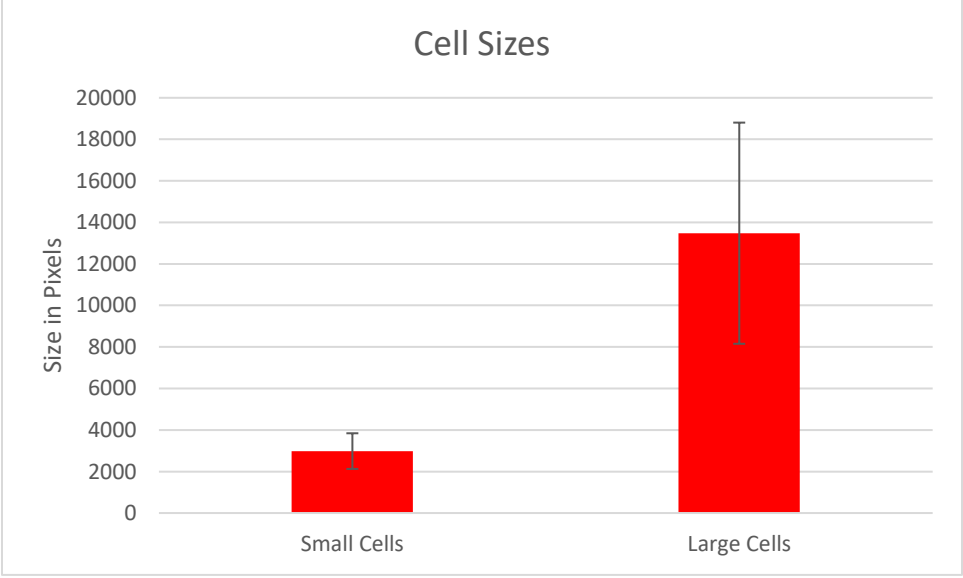

Figure 4.6 Average cell sizes of the two categories of cells from the image analysis

As expected, the small cells were much smaller than the large cells. That said, the cell sizes are not statistically different despite visually appearing so. This is mostly due to the high variance of the large cells. Dividing the nuclei sizes by the cell sizes gives the nuclear-cytoplasmic ratio. The results for the ratios are shown in the graph below (Figure 4.7).

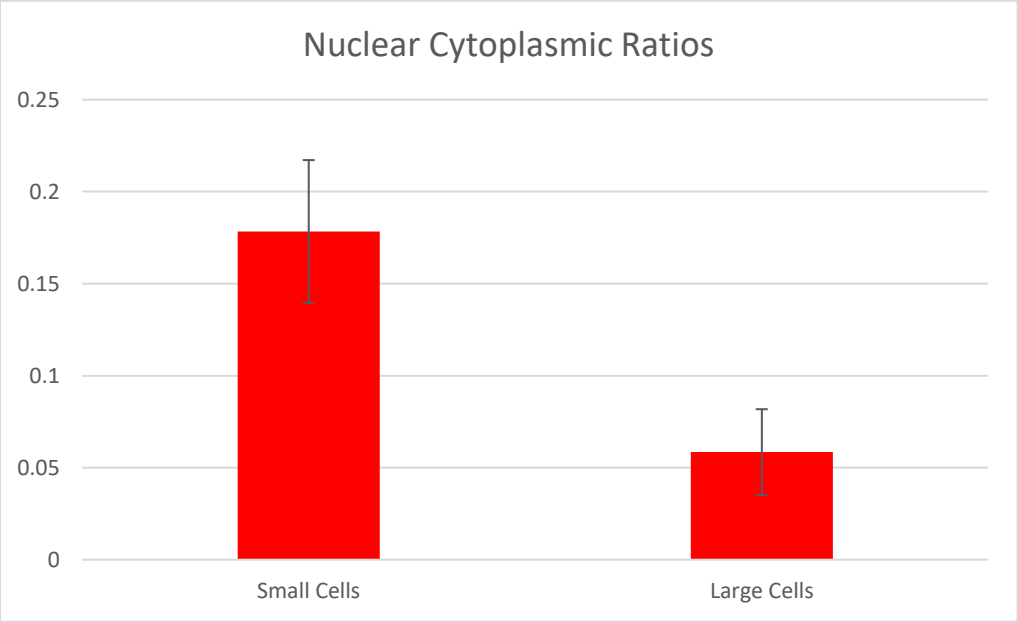

Figure 4.7 Average cell sizes of the two categories of cells from the image analysis

The small cells had a much higher nuclear-cytoplasmic ratio than the large cells as anticipated. When comparing the means, they were statistically significantly different at a .01 level with a p value of 0.00006. This confirms the heterogeneity of the ratios.

4.4 Summary and Future Work

The heterogeneity of mice CPECs were explored using microscope imaging. Images of P21 CPEC monolayers were taken to analyze their size and morphology.The epifluorescent images showed various cell morphologies and some smaller cells being enveloped by larger cells. These

small enveloped cells were compared to the other cells to determine the heterogeneity of the nuclear-cytoplasmic ratios. Image analysis was performed to determine the relative sizes of the nuclei and cytoplasm to calculate the ratios. It was determined that the nuclei did not vary in size between these two groups but the nuclear-cytoplasmic significantly differed. This kind of analysis can be done on in situ samples to determine the heterogeneity present in the intact cells in comparison to those in primary cell culture. Future studies can tie the results of this analysis to CPEC phenotypes to determine how the morphologies and nuclear-cytoplasmic ratios affect CPEC expression.

CHAPTER 5: CPEC Protein Expression

5.1 Heterogeneity in CPEC Protein Expression Heterogeneity

In the previous chapter, it became apparent that heterogeneity was prominent in the transgenic mice primary culture. The nucleus to cytoplasmic ratio of large cells compared to small cells was statistically significantly different at a .01 level with a p value of 0.00006. Given these differences, this study sought to reveal more cellular differences. Immunohistochemistry and flow cytometry assays were conducted to determine if heterogeneity in protein expression existed. The protein that was studied was Aquaporin 1. Since Aquaporin 1 water channels are found throughout the cell membrane, it was hypothesized that Aquaporin 1 expression would be significantly heterogeneous because the nucleus to cytoplasmic ratio varied in culture. It was hypothesized that the smaller cells would express less Aquaporin 1 than the large cells, as their nucleus to cytoplasmic ratio is large which means that there is less water to pump out of the cells which means fewer aquaporins are needed to maintain homeostasis.

5.2 Cell Expression Heterogeneity Methods

5.2.1 Dissection and Cell Culture

Primary cultures of epithelial cells from mouse CPECs were prepared using the following method. Three-week old mice were sacrificed using carbon dioxide asphyxiation followed by decapitation. The brains were then exposed and CPEC from all ventricles was dissected using a stereomicroscope. The tissue was then collected and submerged into 500 ul of PBS on ice, until the last CPEC was obtained. Once all the CPEC from lateral and fourth ventricles had been pooled, 500ul of collagenase II with 3mM were added to dissociate the tissue. The PBS/Collagenase II+Ca2 mixture was then put an incubator at 37C for 45 minutes. To ensure dissociation was adequate, the CPEC was mechanically dissociated by tapping the eppendorf tube every 5 minutes. The mixture was then centrifuged (3000 rpm for 3 minutes). Following centrifugation step, the pellet of cells was washed with CPEC media and resuspended. CPEC media is composed of

DMEM supplemented with 10% FBS, 100 units penicillin per mL, 100 pg streptomycin per mL, and 20 µl cytosine arabinoside. Cells were maintained at 37°C, 5% CO_2 on Poly-L-lysine and laminin coated culture wells, and the medium was changed every 72 hours.

5.2.2 Immunohistochemistry

For immunocytochemical examination Aquaporin 1 expression, CP cell cultures were washed with PBS and fixed in 4% paraformaldehyde (PFA) (30 minutes) followed by three washes with PBS. The wells were rinsed with 0.05% Triton X-100 and blocked with 1% bovine serum albumin (BSA) in PBS (45 minutes) prior to incubation with a 1:500 dilution of the primary antibody. Following incubation with the primary antibody for 60 minutes at 37°C, the cultures were incubated in the dark with a fluorescence labeled goat anti-rabbit IgG antibody. for 45 minutes at 37°C. Finally, the cells were washed in PBS solution and mounted for microscopic visualization.

5.2.3 Flow Cytometry

TTR:tdTomato CPEC cells were collected and dissociated using the primary cell culture method mentioned in previous chapter. Following centrifugation (3000 rpm/3 minutes), the supernatant was aspirated, and 500 µL of 0.01% paraformaldehyde was added to each tube and left for 10 minutes. The cells were washed and resuspended in 0.04% Triton X-100, and the samples were separately incubated with 100µLof Aquaporin 1 primary antibodies (diluted 1:100 in blocking buffer BSA/PBS 3%) overnight at 4°C. Cells were then washed with PBS and centrifuged at 3000 rpm for 3minutes. These cells were later incubated in the dark with 100 µL of fluorescent goat anti-rabbit secondary antibody (diluted 1:100 in blocking buffer BSA/PBS 3%) for 45 minutes at 37°C. After washing with PBS and centrifugation at 3000 rpm for 3 minutes, 500 µL of PBS was added to each tube and the samples were immediately subjected to measurement by a Becton Dickinson Fluorescence- activated cell Scan analyzer.

5.3 Protein Cell Expression Results

5.3.1 Immunohistochemistry Results

In the Figure 5.1 below, an epifluorescence image of P21 CPEC primary culture is shown. Upon first observations, heterogeneity in Aquaporin1 is boldly illustrated. Amongst the cuboidal CPECs, Aquaporin1 had a wide range of distribution and level. In some cells, very little Aquaporin1 is expressed and the expression is irregular. In other cells, Aquaporin1 is abundantly expressed. Using ImageJ, the cell's intensity was measured. The brightest cells had an intensity that was twofold greater the darkest cells.

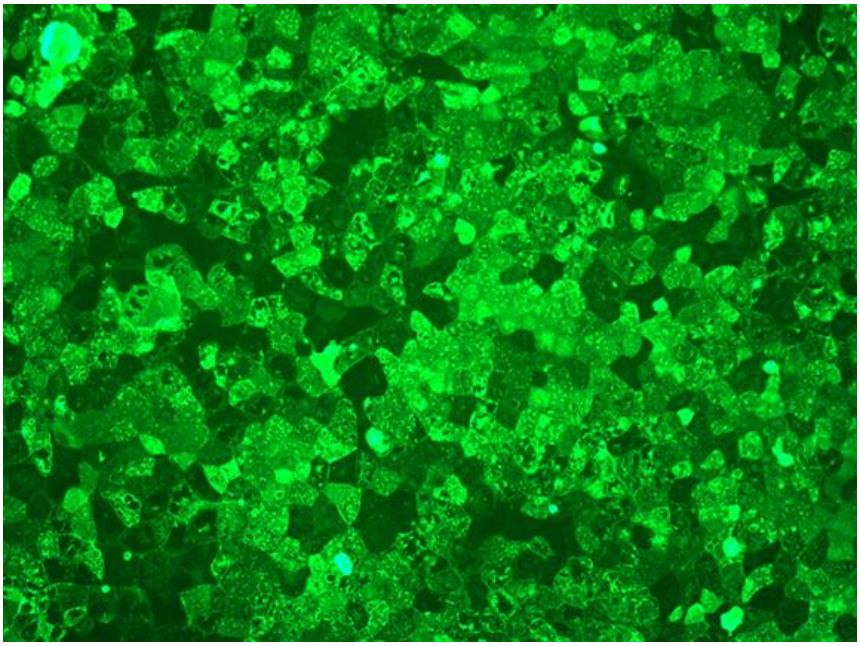

Figure 5.1 The epifluorescent microscope micrograph in the figure below shows the confluent monolayer of P21 mouse CP epithelial cells after three weeks of culture in 10% FBS/DMEM. Green is Aquaporin 1.

To further assess Aquaporin1 expression heterogeneity, flow cytometry was performed. Flow cytometry allows a sample of cells or particles in suspension to be separated through a narrow, rapidly flowing stream of liquid. As the sample passes through, a laser allows for detection of size, granularity, and fluorescent properties of individual cells/particles in the sample. In this way, a composition of heterogeneous biological samples may be de-convoluted. By using

fluorescently labeled antibodies targeting Aquaporin 1, information regarding CPEC composition was extracted.

5.3.2 Determining Aquaporin1 Fluorescence baseline

To determine the fluorescence patterns of Aquaporin 1, it was imperative to first determine if CPEC cells were naturally autofluorescence. A control sample of TTR:tdTomato negative CPEC cells underwent flow cytometry analysis. The suspension contained CPEC pooled from 10 P21 TTR:tdTomato negative mice which resulted in approximately 300,000 cells.

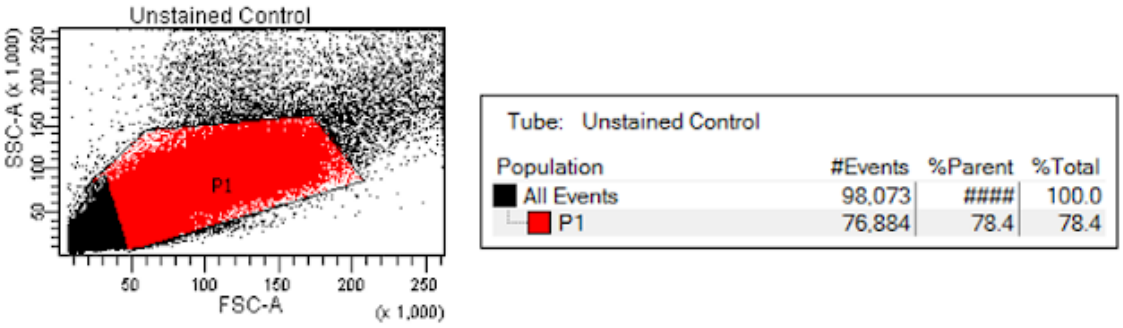

Figure 5.2 Aquaporin 1 flow cytometry in choroid plexus epithelial cells. A) Flow cytometry dot plot from single cell suspicion of pooled CPEC not labelled with antibodies. B) The Aquaporin 1 negative control had 78% viability.

As seen in Figure 5.2, choroid plexus cells are quite robust. Despite having undergone long incubation periods, staining, and flow cytometry, the cells exhibited 78% viability. This was an important discovery, as CPEC flow cytometry was not previously achieved in mice older than P8. This was most likely due to the harsh conditions needed to dissociate CPEC tight junctions. To reduce CPEC stress and improve viability, this study changed the dissociation protocol. The PBS/Collagenase II+Ca2 mixture was diluted and the sample was placed in an incubator at 37C

up throughout dissociation. Once thoroughly dissociated, the sample was placed in ice until the flow cytometry commenced.

Once the viability of the cells proved to be adequate, Aquaporin1 levels and thresholds were detected. As seen in Figure 5.3, the samples were tested for mCherry and APC fluorescence. APC fluorescence was tested because that is the filter that detected the Aquaporin1 antibody. mCherry was selected because the filter detects red cells. If future studies wanted to compare TTR:tdTomato expression with the Aquaporin1, this value would be required.

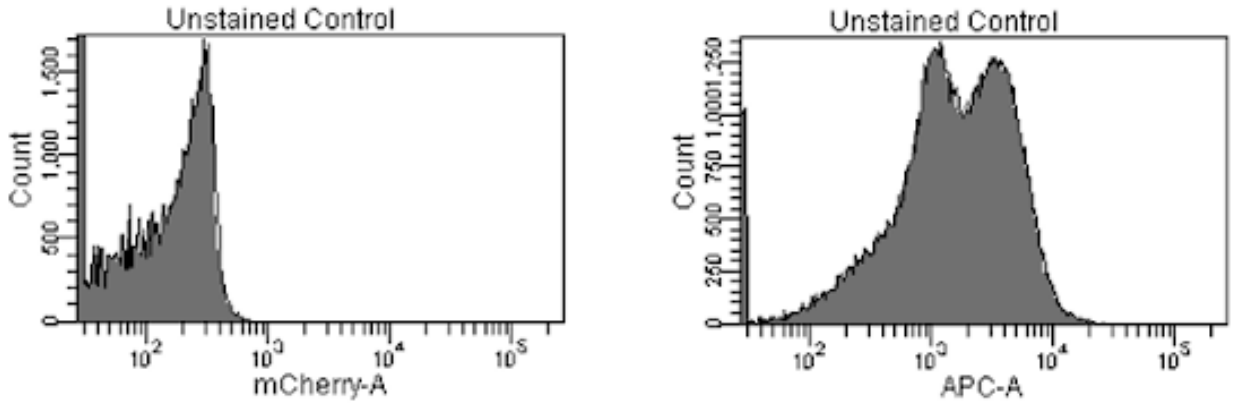

Figure 5.3 Aquaporin 1 flow cytometry in choroid plexus epithelial cells. A) Flow cytometry histogram data of a single suspicion. mCherry intensity is seen in the horizontal axis B) Flow cytometry histogram data of single suspension. APC intensity is horizontal axis.

5.3.3 Aquaporin1 Stained Sample

Control sample thresholds were used as boundary conditions for the test sample. The test sample was an Aquaporin 1 stained suspension. The suspension was comprised of CPEC pooled from 10 P21 TTR:tdTomato negative mice which resulted in approximately 300,000 cells. As seen

in Figure 5.4, these cells were slightly less viable than the control. 70.2% viability was observed in comparison to the 78% in the control.

Tube: APC Stained Control

Population	#Events	%Parent	%Total
All Events	85,589	####	100.0
P1	60,079	70.2	70.2
P2	59,699	99.4	69.8

Figure 5.4 Aquaporin 1 flow cytometry in choroid plexus epithelial cells. A) The Aquaporin 1 test sample had 70% viability.

As seen in Figure 5.5, Aquaporin 1 had a clear fluorescent pattern, and Aquaporin 1 was expressed in almost every single cell (99.4%). Given these results, Aquaporin 1 can be used as a CPEC marker in future flow cytometry studies.

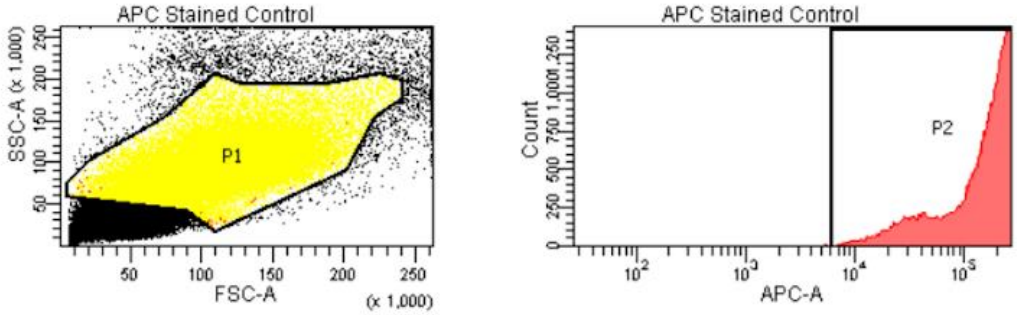

Figure 5.5 Aquaporin 1 flow cytometry in choroid plexus epithelial cells. A) Flow cytometry dot plot from single cell suspicion of pooled CPEC labelled Aquaporin 1 with antibodies. B) Flow cytometry histogram data of single suspension. APC intensity is horizontal axis.

5.4 Conclusion and Future Work

Cells were stained with the primary antibody followed by FITC conjugated secondary antibody and analyzed with a flow cytometer. The Aquaporin negative control had 78% viability; while the control sample exhibited 70% viability. From the test sample, it was determined that Aquaporin1 expression in CP cells is 99.4% and that there is a large distribution in intensity across cells. In the future, it would be interesting to do the previous experiment with TTR:tdTomato positive cells in order to correlated TTR expression with Aquaporin1. Furthermore, it would be interesting to compare Aquaporin1 expression with other water transport proteins in the choroid plexus. Perhaps, the reason heterogeneity is abundant in Aquaporin1 expression is because there are other proteins that counteract high/low levels of this water channel, thus allowing CSF production to remain consistent in the body.

CHAPTER 6: Transwell CPEC Culture

6.1 Introduction

One of the key properties of the choroid plexus is its barrier-like structure. The CPEC joined by tight junction form the blood cerebrospinal fluid barrier, one of the most important barriers in the human body. To provide a baseline of this barrier's integrity in vitro, transepithelial electrical resistance (TEER) values were measured. TEER is a widely accepted quantitative technique to measure barrier properties in cell culture models of endothelial and epithelial monolayers. TEER values are strong indicators of the integrity of the cellular barriers before they are evaluated for transport of drugs or chemicals. Due to the anatomical location of the CP, there is no data on TEER in vivo available for mammals and no TEER information on lateral CP TEER for any species. In primary cultures of rat CPEC, TEER values were in the range of 100–500 Ωcm2. Porcine CPEC models displayed resistance values in the range of 100 to 170 Ωcm2. (Baehr et al., 2006)Values for mouse CPEC TEER were not found. This study aimed to fill this gap by providing TEER values of both the lateral and fourth ventricle CPEC primary cultures.

To calculate TEER, the transcellular pathway resistance value was divided by the paracellular pathway resistance. The transcellular pathway Rtrc, is the sum of the apical cell membrane resistance (Ra) and the basolateral cell membrane resistance (Rb). Rpc depicts the paracellular pathway and is equal to the sum of the tight junction resistance (Rtj) and the intercellular resistance (Ric).

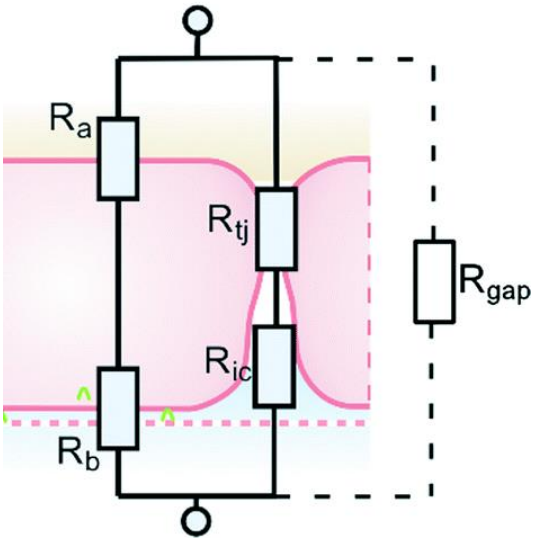

$$T_{TEER} = R_{tre} // R_{pc} = \frac{(R_A + R_B)\cdot(R_{tj} + R_{ic})}{(R_A + R_B) + (R_{tj} + R_{ic})}$$

Figure 6.1 Schematic of TEER and the formula used to calculate TEER

6.2 Measuring Transepithelial Electrical Resistance (TEER) in Transwells

TEER values were determined for CPEC grown on permeable polyester Costar Transwell® membranes, using the Millicell®-ERS and STX-2 electrode system (World Precision Instruments, Berlin, FRG). Control values obtained from coated filters without cells (blank) were subtracted and the resulting values multiplied by the filter surface area, resulting in TEER values of Ωcm2.

6.3 TEER Results

TEER values have been used extensively as a measure for leakiness of cellular barriers. In the present study, CPEC monolayers displayed TEER values in the 100 Ωcm2 range and were judged confluent after 48hrs in culture. After 8 days in culture, the CPEC monolayer that had been grown in media with bovine serum and the monolayer that had no serum both had TEER values of 247 Ωcm2. Similarly, after 11 days in culture, both continued to produce the same results – each transwell had TEER values of 263 Ωcm2. This result was unexpected as serum has been shown to affect barrier formation. In brain capillary endothelial cells, serum has prevents tight junction formation which results in a decrease in TEER values. (Srinivasan et al., 2015). This suggests that

the experimental set up should be revisited in the future to determine if improper tools caused this discrepancy.

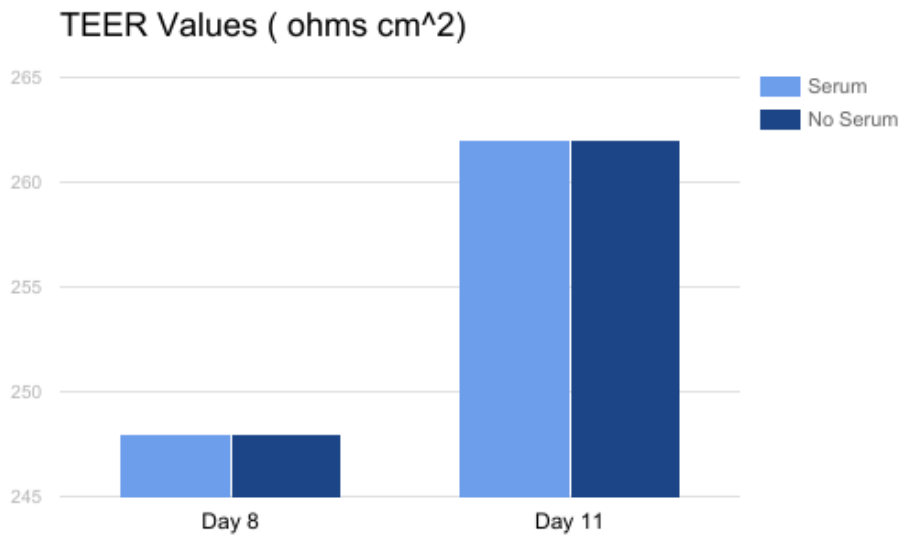

Figure 6.2 Choroid Plexus monolayer transwell cultures were cultivated with and without bovine serum. After 8 and 11 days, TEER values were collected.

6.4 Summary and Future Work

The choroid plexus TEER values in the mouse reporter line primary cultures was in the appropriate range for mammalian epithelial barriers. That said, the TEER values were consistent in both serum and serum-free cultures, suggesting that the TEER calculation may not be accurately depicting the CPEC's resistance. In order to the obtain more faithful results, CPEC TEER calculations should be conducted at more regular intervals. Furthermore, the CPEC from the new reporter mouse line should be used as well. Since CPEC in the transgenic mouse line is fluorescent, if images of the fluorescent line were to be taken in parallel with the TEER value measurements, we would be able to correlate the TTR expression, the health of the cell, and the TEER values.

This future experiment could shed light into the mechanisms of CSF secretion and potential uncover correlations with TTR synthesis. Furthermore, it may shed light into potential drug delivery pathways. Using the data extrapolated from the TEER values, a decrease in TEER could present an opportunity for drug delivery. That said, more research needs to be conducted in order for in vitro conditions to mimic the in vivo barriers. Without proper reproduction of in vivo conditions, TEER values will not be able to accurately model drug absorption and secretion accurately.

CHAPTER 7: Conclusion and Future work

This body of work focused on the choroid plexus. In Chapter 1, the choroid plexus was defined, and two of its primary roles were studied: 1) secretion and 2) its barrier properties. As was previously mentioned, the choroid plexus is responsible for producing CSF; it is estimated that 70% of CSF production occurs in the choroid plexus. CSF keeps the brain nourished by circulating nutrients and removing metabolic wastes. Inconsistencies in CSF production have been linked to numerous brain pathologies, from Aβ and Biondi ring tangles accumulation in Alzheimer's disease and other neurodegenerative conditions.

In Chapter 2, the choroid plexus epithelial cells (CPEC) were introduced along with their morphology. Briefly, the CPEC are responsible for the choroid plexus' barrier and CSF producing properties. These sturdy cells have a basal and apical side. The basal side surrounds fenestrated capillaries which allow immune cells, proteins, and small molecules to enter the choroid plexus. The apical sides work as a barrier that limits entry into the CNS and pumps CSF into the ventricles. These cells form the blood-brain barrier and keep the brain healthy and nourished.

Given the immense effect these cells have on the central nervous system, this thesis dove into further detail and examined these cells at the cellular level. To conduct this analysis, a reporter mouse line was designed by our lab and created with the help of the UCI transgenic mice facility. The transgenic mice had a BAC inserted containing the tdTomato protein coding sequence inserted into the human *Transthyretin* gene. Since Transthyretin is ubiquitous in CPEC and specific to the choroid plexus, our lab expected the reporter to faithfully identify CPEC. (Johnson et al., 2018) Our hypothesis was correct. Upon brain dissection, it was evident that the CPEC fluoresced bright red in the TTR:tdTomato genotypically positive mice. Furthermore, when this line was bred and

produced homozygous mice, the mice were healthy and viable, suggesting that this homozygous reporter line can be used in the future studies to accurately study the CPEC.

In Chapter 4 and Chapter 5, the TTR:tdTomato reporter mouse line was used to study the CPEC at a cellular level. CPEC from 4th and lateral ventricles of P21 mice were dissected and cultured. After 48 hours a monolayer formed, and after a week in culture the cells were underwent immunohistochemistry and flow cytometry analysis. After staining the primary cells, it was clear that the CPEC were highly heterogeneous. Epifluorescent images show various cell morphologies: there are small cells being enveloped by larger cells and large cuboidal shaped cells. To compare the cells, nuclear-cytoplasmic ratios were calculated. It was determined that the nuclei did not vary in size between these two groups, but nuclear-cytoplasmic ratios significantly differed. The small cells had a much higher nuclear-cytoplasmic ratio than the large cells.

These quantifiable differences posed new questions. Could this heterogeneity be seen in other cell properties? Specifically, could this heterogeneity lead to protein expression differences? To begin to answer this question this study performed flow cytometry analysis. The protein of choice was Aquaporin1. Aquaporin1 is a membrane protein localized on the apical side of the CPEC. Previous Aquaporin1 studies suggest that it functions as a gated water channel, and it is believed that ionic conductance can significantly regulate CSF secretion. In this study, the Aquaporin1 negative control had 78% viability; while the control sample exhibited 70% viability. From the test sample, it was determined that Aquaporin1 expression in CP cells is 99.4% and that the there is a large distribution in intensity across cells. More experiments will need to be conducted to improve viability.

Once flow cytometry protocols for CPEC are established, a variety of experiments can be conducted. If this study could be extended, it would begin by comparing Aquaporin1 to

TTR:tdTomato. By comparing TTR expression to Aquaporin1, one would be able to determine what percentage of CPEC express Aquaporin1, not just what percentage of choroid plexus cells express Aquaporin1.

Since the mechanisms by which CPEC produce CSF and pump water is not clearly understood, another experiment that could be performed is the comparison of Aquaporin1 to other transport proteins in CPEC. In recent studies, it was determined that transport protein, nkcc1, could pump water out of CPEC without the need of an osmotic gradient. (Gregoriades et al., 2019) It would be interesting to see if there exist a correlation between Aquaporin1 and nkcc1. Perhaps, in cells where less Aquaporin1 is expressed nkcc1 is seen in abundance, and vice versa.

CPEC heterogeneity should not be limited to flow cytometry and image analysis. Given the lack of knowledge and variety observed, this study, if extended, would focus on integrative methods for single cell analysis. To begin, this study would use single-cell transcriptome analysis to identity distinct cell types at critical periods of CPEC development. In the mouse brain, choroid plexus specification occurs between E8 and E9 days. Thus, one of the first data points would be gather in E9 mice. The second data point would be gathered at P0 to compare cell types at birth. P21 would be the third point to see if the same cell types continue to be present when mice have reached young adult. To end the longevity study, the single-cell transcriptome analysis would be conducted when mice have reached adulthood. This should provide a holistic view of the various CPEC cell types and their respective ratios throughout the mouse's life cycle.

Since the mechanisms behind CPEC function remain a mystery, it would be beneficial to use the single cell experiments to find correlations between its results and the functional properties of the choroid plexus. As discussed in Chapter 6, the CPEC's barrier properties are vital, and the best way to study barriers is by studying barrier integrity. The TEER study performed as part of this

thesis should be expanded. After identifying TEER values at more regular intervals starting at 48hrs post dissection and establishing a baseline for primary mouse CPEC culture, one can then perform drug studies to determine if there are correlations between barrier integrity and protein expression; thereby, linking subcellular properties with tissue properties.

In conclusion, this study determined that CPEC are highly heterogenous. This heterogeneity could affect the functionality of these cells which can be explored in future studies. The methods used in this study would be used on CPEC alongside analysis of choroid plexus tissue to assess the link between heterogeneity and tissue properties. This study also introduced a new tool, the TTR:tdTomato reporter mouse line, to conduct these studies that could pave the way for CPEC translational work. With more tools for analyzing the connections between cells and tissues, the mysteries of the choroid can soon be unraveled.

REFERENCES

Altschuler, S. J., & Wu, L. F. (2010). Cellular Heterogeneity: Do Differences Make a Difference? *Cell*, *141*(4), 559–563. https://doi.org/10.1016/j.cell.2010.04.033

Baehr, C., Reichel, V., & Fricker, G. (2006). Choroid plexus epithelial monolayers - A cell culture model from porcine brain. *Cerebrospinal Fluid Research*, *3*, 13. https://doi.org/10.1186/1743-8454-3-13

Barkho, B. Z., & Monuki, E. S. (2015). Proliferation of cultured mouse choroid plexus epithelial cells. *PLoS ONE*, *10*(3). https://doi.org/10.1371/journal.pone.0121738

Boassa, D., & Yool, A. J. (2005). *Physiological Roles of Aquaporins in the Choroid Plexus*. https://doi.org/10.1016/S0070-2153(04)67005-0

Chang, A. Y., & Marshall, W. F. (2017). Organelles - Understanding noise and heterogeneity in cell biology at an intermediate scale. *Journal of Cell Science*, *130*(5), 819–826. https://doi.org/10.1242/jcs.181024

Choroid Plexus Tumors - National Cancer Institute. (n.d.). Retrieved January 12, 2020, from https://www.cancer.gov/rare-brain-spine-tumor/tumors/choroid-plexus-tumors

Gabrion, J. B., Herbuté, S., Bouillé, C., Maurel, D., Kuchler-Bopp, S., Laabich, A., & Delaunoy, J. P. (1998). Ependymal and choroidal cells in culture: Characterization and functional differentiation. *Microscopy Research and Technique*, *41*(2), 124–157. https://doi.org/10.1002/(SICI)1097-0029(19980415)41:2<124::AID-JEMT3>3.0.CO;2-U

Good, M. C. (2015). Turn Up the Volume: Uncovering Nucleus Size Control Mechanisms. *Developmental Cell*, *33*(5), 496–497. https://doi.org/10.1016/j.devcel.2015.05.015

Gregoriades, J. M. C., Madaris, A., Alvarez, F. J., & Alvarez-Leefmans, F. J. (2019). Genetic and pharmacological inactivation of apical Na+-K+-2Cl- cotransporter 1 in choroid plexus epithelial cells reveals the physiological function of the cotransporter. *American Journal of Physiology - Cell Physiology*, *316*(4), C525–C544. https://doi.org/10.1152/ajpcell.00026.2018

Javed, K., & Lui, F. (2019). Neuroanatomy, Choroid Plexus. In *StatPearls*. StatPearls Publishing. http://www.ncbi.nlm.nih.gov/pubmed/30844183

Jevtić, P., Edens, L. J., Vuković, L. D., & Levy, D. L. (2014). Sizing and shaping the nucleus: Mechanisms and significance. *Current Opinion in Cell Biology*, *28*(1), 16–27. https://doi.org/10.1016/j.ceb.2014.01.003

Johanson, C. E., & Johanson, N. L. (2018). Choroid Plexus Blood-CSF Barrier: Major Player in Brain Disease Modeling and Neuromedicine. In *J Neurol Neuromedicine* (Vol. 3, Issue 4). www.jneurology.comNeuromedicine

Johnson, B. A., Coutts, M., Vo, H. M., Hao, X., Fatima, N., Rivera, M. J., Sims, R. J., Neel, M. J., Kang, Y.-J., & Monuki, E. S. (2018). Accurate, strong, and stable reporting of choroid plexus epithelial cells in transgenic mice using a human transthyretin BAC. *Fluids and Barriers of the CNS*, *15*(1), 22. https://doi.org/10.1186/s12987-018-0107-4

Lobas, M. A., Helsper, L., Vernon, C. G., Schreiner, D., Zhang, Y., Holtzman, M. J., Thedens, D. R., & Weiner, J. A. (2012). Molecular heterogeneity in the choroid plexus epithelium: The 22-member γ-protocadherin family is differentially expressed, apically localized, and implicated in CSF regulation. *Journal of Neurochemistry*, *120*(6), 913–927. https://doi.org/10.1111/j.1471-4159.2011.07587.x

Lun, M. P., Johnson, M. B., Broadbelt, K. G., Watanabe, M., Kang, Y. J., Chau, K. F., Springel, M. W., Malesz, A., Sousa, A. M. M., Pletikos, M., Adelita, T., Calicchio, M. L., Zhang, Y., Holtzman, M. J., Lidov, H. G. W., Sestan, N., Steen, H., Monuki, E. S., & Lehtinen, M. K. (2015). Spatially heterogeneous choroid plexus transcriptomes encode positional identity and contribute to regional CSF production. *Journal of Neuroscience*, *35*(12), 4903–4916. https://doi.org/10.1523/JNEUROSCI.3081-14.2015

Mastorakos, P., & McGavern, D. (2019). The anatomy and immunology of vasculature in the central nervous system. In *Science Immunology* (Vol. 4, Issue 37). American Association for the Advancement of Science. https://doi.org/10.1126/sciimmunol.aav0492

Richardson, S. J., Wijayagunaratne, R. C., D'Souza, D. G., Darras, V. M., & Van Herck, S. L. J. (2015). Transport of thyroid hormones via the choroid plexus into the brain: The roles of transthyretin and thyroid hormone transmembrane transporters. In *Frontiers in Neuroscience* (Vol. 9, Issue MAR). Frontiers Media S.A. https://doi.org/10.3389/fnins.2015.00066

Spector, R., Keep, R. F., Robert Snodgrass, S., Smith, Q. R., & Johanson, C. E. (2015). A balanced view of choroid plexus structure and function: Focus on adult humans. In *Experimental Neurology* (Vol. 267, pp. 78–86). Academic Press Inc. https://doi.org/10.1016/j.expneurol.2015.02.032

Srinivasan, B., Kolli, A. R., Esch, M. B., Abaci, H. E., Shuler, M. L., & Hickman, J. J. (2015). TEER Measurement Techniques for In Vitro Barrier Model Systems. In *Journal of Laboratory Automation* (Vol. 20, Issue 2, pp. 107–126). SAGE Publications Inc. https://doi.org/10.1177/2211068214561025

Stauder, A. J., Dickson, P. W., Aldred, A. R., Schreiber, G., Mendelsohn, F. A., & Hudson, P. (1986). Synthesis of transthyretin (pre-albumin) mRNA in choroid plexus epithelial cells, localized by in situ hybridization in rat brain. *Journal of Histochemistry and Cytochemistry*, *34*(7), 949–952. https://doi.org/10.1177/34.7.3458812

Suzuki, Y., Nakamura, Y., Yamada, K., Igarashi, H., Kasuga, K., Yokoyama, Y., Ikeuchi, T., Nishizawa, M., Kwee, I. L., & Nakada, T. (2015). Reduced CSF Water Influx in Alzheimer's Disease Supporting the β-Amyloid Clearance Hypothesis. *PLOS ONE*, *10*(5), e0123708. https://doi.org/10.1371/journal.pone.0123708

Vieira, M., Gomes, J. R., & Saraiva, M. J. (2015). Transthyretin Induces Insulin-like Growth Factor I Nuclear Translocation Regulating Its Levels in the Hippocampus. *Molecular Neurobiology*, *51*(3), 1468–1479. https://doi.org/10.1007/s12035-014-8824-4

Vuković, L. D., Jevtić, P., Edens, L. J., & Levy, D. L. (2016). New Insights into Mechanisms and Functions of Nuclear Size Regulation. *International Review of Cell and Molecular Biology*, *322*, 1–59. https://doi.org/10.1016/bs.ircmb.2015.11.001

Watanabe, M., Kang, Y. J., Davies, L. M., Meghpara, S., Lau, K., Chung, C. Y., Kathiriya, J., Hadjantonakis, A. K., & Monuki, E. S. (2012). BMP4 sufficiency to induce choroid plexus epithelial fate from embryonic stem cell-derived neuroepithelial progenitors. *Journal of Neuroscience*, *32*(45), 15934–15945. https://doi.org/10.1523/JNEUROSCI.3227-12.2012

Webster, M., Wikin, K. L., & Cohen-Fix, O. (2009). Sizing up the nucleus: Nuclear shape, size and nuclear-envelope assembly. *Journal of Cell Science*, *122*(10), 1477–1486. https://doi.org/10.1242/jcs.037333

Wen, G. Y., Wisniewski, H. M., & Kascsak, R. J. (1999). Biondi ring tangles in the choroid plexus of Alzheimer's disease and normal aging brains: A quantitative study. *Brain Research*, *832*(1–2), 40–46. https://doi.org/10.1016/S0006-8993(99)01466-3

Wright, C. A., Path, F. R. C., Burg, M. Van Der, Ph, D., Geiger, D., & Sc, M. (2008). Diagnosing Mycobacterial Lymphadenitis in Children Using Fine Needle Aspiration Biopsy : Cytomorphology , ZN Staining and Autofluorescence — Making More of Less. *Diagnostic Cytopathology*, *36*(4), 245–251. https://doi.org/10.1002/dc

Zhao, Y.-Z., Lu, C.-T., Li, X.-K., & Cai, J. (2013). Ultrasound-mediated strategies in opening brain barriers for drug brain delivery. *Expert Opinion on Drug Delivery*, *10*(7), 987–1001. https://doi.org/10.1517/17425247.2013.787987